Wavelength Reuse in a UWB Over WDM-PON Based on Injection Locking of a Fabry–Pérot Laser Diode and Polarization Multiplexing

Wentao Cui, *Student Member, IEEE*, Tong Shao, *Member, IEEE*, and Jianping Yao, *Fellow, IEEE*

***Abstract*—Wavelength reuse in a symmetric ultra-wideband (UWB) over wavelength-division-multiplexing passive optical network based on injection locking of a Fabry–Pérot laser diode (FP-LD) and polarization multiplexing is proposed and experimentally demonstrated. In the proposed scheme, the downstream UWB signal and baseband signal are generated and polarization multiplexed in the central station and sent to a base station (BS) over an optical fiber. At the BS, one of the downstream signals is selected to injection lock the FP-LD. It is demonstrated theoretically and experimentally that the upstream service performance is less sensitive to the modulation depth of the downstream UWB signal than the baseband signal, and the use of the downstream UWB signal as the injection signal would contribute to a better transmission performance for both the downstream and upstream services. Thus, the downstream UWB signal is selected as the injection signal. An experiment is performed. When the FP-LD is injection locked by a downstream UWB signal, a clear optical carrier is generated which is reused for upstream UWB and baseband transmission. A bidirectional point-to-point transmission of 1.25 Gb/s UWB signal and 10 Gb/s baseband signal over 25-km single-mode fiber using a single wavelength is demonstrated. The bit error rate performances and the eye diagrams for both downstream and upstream transmissions are measured.**

***Index Terms*—Fabry–Pérot laser diode (FP-LD), injection locking, passive optical network (PON), polarization multiplexing, ultra-wideband over fiber, wavelength-division-multiplexing (WDM), wavelength reuse.**

I. Introduction

Ultra-wideband (UWB) was proposed to provide low-complexity, low-cost, low-power consumption, and high-data-rate wireless connectivity for wireless local-area network and personal-area network applications [1]. Based on the definition by the US Federal Communications Commission (FCC), the frequency band assigned to UWB indoor communications systems extends from 3.1 to 10.6 GHz, with a bandwidth of 7.5 GHz centered around 7 GHz. The power spectral density (PSD) is limited to –41.3 dBm/MHz. Due to the low PSD, UWB communications can co-exist with other conventional wireless communications with negligible interferences [1], but the transmission distance is limited to a few to tens of meters. To extend the area of coverage and integrate UWB services into fixed wired or wireless communications networks, a solution is to distribute UWB signals over optical fibers or UWB over fiber [2].

On the other hand, fixed fiber deployments for fiber to the home (FTTH) services are increasing. Passive optical network (PON) technology is the leading FTTH technology, including Gigabit PON and Ethernet PON, both are based on time-division multiple access, providing services to N users by use of passive $1{:}N$ power splitters with an aggregate bit rate. These techniques, however, are regarded to not be able to keep up with the requirements for future access networks regarding aggregated bandwidth, attainable reach, and allowable power budget [3]. These problems can be mitigated by assigning an individual wavelength to each optical network unit (ONU). The architecture, referred to as a wavelength division multiplexing PON (WDM-PON), is attractive due to the advantages, such as increased per ONU bandwidth, reduced optical splitting loss, point-to-point connectivity, protocol agnosticism, bit-rate transparency, large scalability, and high flexibility [4]. In a WDM-PON, multiple light sources and wavelength selective components with high wavelength precision are needed, which may increase the system complexity and cost [5]. To simplify the operation, ease the maintenance and reduce the cost, wavelength reuse has been proposed as an effective solution to realize a "colorless" ONU [4]. Among the various wavelength reuse schemes, injection locking of a Fabry–Pérot laser diode (FP-LD) [6]–[9], gain-saturation of a reflective semiconductor optical amplifier [10]–[13] and the utilization of a separated optical carrier for uplink connection [14]–[17] have been considered the three major solutions and have been widely investigated. However, it should be noted that for the schemes using injection locking of an FP-LD, the commonly utilized downstream injection optical signal is a baseband signal. The limitation of such an injection locking method is that the performance of the upstream signal is sensitive to the modulation depth or extinction ratio (ER) of the downstream signal. When the modulation depth of the downstream baseband signal increases, the injection-locked optical carrier at the output of the FP-LD is severely degraded, which is not suitable for upstream data re-modulation. Therefore, there is an obvious tradeoff between the ER of the downstream signal and the performance of the upstream signal.

In this paper, a wavelength reuse scheme for symmetric UWB over WDM-PON based on injection locking of an FP-LD and polarization multiplexing is proposed and experimentally

Manuscript received May 18, 2013; revised August 27, 2013; accepted September 24, 2013. Date of publication September 29, 2013; date of current version December 11, 2013. This work was supported by the Natural Sciences and Engineering Research Council of Canada (NSERC).

The authors are with the Microwave Photonics Laboratory, School of Electrical Engineering and Computer Science, University of Ottawa, Ottawa, ON K1N 6N5, Canada (e-mail: jpyao@eecs.uOttawa.ca).

Color versions of one or more of the figures in this paper are available online at http://ieeexplore.ieee.org.

Digital Object Identifier 10.1109/JLT.2013.2283776

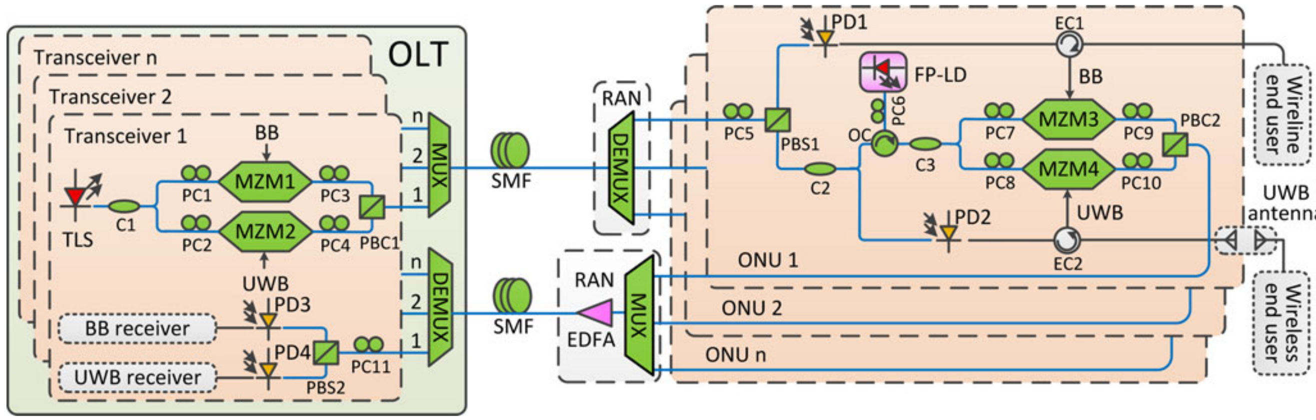

Fig. 1. The proposed UWB over WDM-PON architecture with wavelength reuse based on injection locking of an FP-LD and polarization multiplexing. BB: baseband.

demonstrated. It is different from the previous injection locking schemes where the injection signal is a downstream baseband signal; here, the injection signal is a downstream UWB signal. It is demonstrated here that the injection locking of an FP-LD using a UWB signal would make the upstream service performance less sensitive to the ER of the downstream UWB signal than the baseband signal, and the use of the downstream UWB signal as an injection signal would contribute to better transmission performance for both the downstream and upstream services.

In the proposed system, a pseudorandom bit sequence (PRBS) UWB signal and a PRBS baseband signal are modulated on an optical carrier at two Mach–Zehnder modulators (MZMs) in a transceiver at the optical line terminal (OLT), and are polarization multiplexed. The output signals from the transceivers are wavelength multiplexed and sent to the remote access node (RAN) through an optical fiber. After being distributed to the corresponding ONU, the downstream baseband signal and a portion of the UWB signal are converted to electrical signals. Another portion of the UWB signal is taped and directed to the FP-LD to perform injection locking of the FP-LD to generate a clear optical carrier for upstream data transmission. The upstream UWB and baseband signals are also polarization multiplexed. Therefore, a symmetric UWB over WDM-PON is implemented.

To evaluate the performance of injection locking of the FP-LD, a comparative study is performed in which the injection locking using a baseband and a UWB downstream signal is considered. For both signals having an identical optical injection power and an identical electrical modulation power, injection locking using a UWB signal would provide better performance over the use of a baseband signal. The proposed wavelength reuse scheme for the UWB over WDM-PON system has the following advantages. When the UWB signal and the baseband signal have an identical injected optical power, the downstream UWB signal can have a higher electrical modulation power than that of the baseband signal, without obvious negative impact on the performance of the upstream signal. This, in turn, contributes to a better receiver sensitivity for the downstream UWB service. It is true that there is a tradeoff between the ERs of the downstream and upstream signals for the cases of using either a UWB or a baseband injection signal; however, the utilization of a UWB signal as the injection signal would make the system have a higher tolerance against the power penalty introduced by a relatively higher ER of the downstream signal. Therefore, better performances for both downstream and upstream services of the proposed UWB over WDM-PON can be obtained thanks to this property.

A bidirectional point-to-point transmission of 1.25 Gb/s UWB signal and 10 Gb/s baseband signal over a 25-km single-mode fiber (SMF) is experimentally demonstrated. The performance including the eye diagrams, the bit-error rate (BER), and the power budget is evaluated. An error-free transmission of both downstream and upstream services over a 25-km SMF is achieved. The power penalties due to the wavelength reuse and the polarization multiplexing are measured to be as low as 0.2 dB and 0.3 dB, respectively.

II. Principle

A. System Architecture

The schematic of the proposed UWB over WDM-PON based on injection locking of an FP-LD and polarization multiplexing is shown in Fig. 1. At a transceiver in the OLT, a linearly polarized continuous-wave (CW) light wave emitted from a tunable laser source (TLS) is equally divided into two portions through a 50/50 coupler (C1). Each portion of the CW light wave is sent to an MZM through a polarization controller (PC). As illustrated in Fig. 1, the upper portion of the CW light wave is intensity modulated by a baseband signal coded in a PRBS pattern at the MZM (MZM1), while the lower portion is modulated by a PRBS UWB signal at MZM2. The two intensity modulated signals are then polarization multiplexed at a polarization beam combiner (PBC1) through another two PCs. The optical downstream signals from the transceivers are wavelength multiplexed at a WDM multiplexer (MUX) and then transmitted to the RAN through a length of SMF where they are de-multiplexed by a WDM de-multiplexer (DEMUX). The downstream optical signals are then distributed to the corresponding ONUs.

At each ONU, the downstream baseband signal and the UWB signal are polarization de-multiplexed at a polarization beam splitter (PBS1), as shown again in Fig. 1. The baseband signal is then converted into an electrical signal at PD1 and received by the wireline end user. The downstream wireline service is thus implemented. The UWB signal is divided into two parts through a coupler (C2). The lower part is converted into an electrical signal at PD2 and radiated to the free space through a UWB antenna. The wireless UWB signal can be received by the wireless end user through another UWB antenna. The upper part of the optical UWB signal is applied to an FP-LD through an optical circulator and a PC for injection locking. A clear optical carrier is generated at the output of the FP-LD and is used for upstream signal modulation. Similar to the downstream signal, the upstream signal also consists of a baseband signal and a UWB signal. The clear optical carrier is equally divided into two portions through a coupler (C3) and sent to two MZMs (MZM3 and MZM4), at which the optical carriers are modulated by the upstream baseband and UWB signals, as shown again in Fig. 1. The upstream baseband signal and UWB signal are polarization multiplexed at PBC2, wavelength multiplexed at a MUX, amplified by an erbium-doped fiber amplifier (EDFA) at the RAN, and sent to the OLT through a length of SMF. At the OLT, a DEMUX is utilized to de-multiplex the upstream optical signals and send them to the corresponding transceivers. At each transceiver, the optical upstream signal is polarization de-multiplexed through a PC (PC11) and a PBS (PBS2). The polarization de-multiplexed baseband signal and UWB signal are then converted into electrical signals and detected by the corresponding receivers. Consequently, the simultaneous provision of the upstream wireline and wireless services is realized.

B. Injection Locking of an FP-LD

The downstream signal consists of two polarization multiplexed signals, the baseband and the UWB signals. To evaluate the injection locking performance, we first set the optical powers of the UWB and baseband signals identical. The electrical modulation powers of both signals are also kept identical, but can be tuned at different power levels during the injection locking process.

Mathematically, an amplitude modulated optical signal can be expressed as

$$E_1(t) = A[1 + \beta s(t)] \sin(\omega_s t), \quad (1)$$

where A is the amplitude of the optical carrier, $\beta$is the amplitude modulation index, $s(t)$ is the normalized electrical UWB or baseband modulation signal, and ω_s is the angular frequency of the optical carrier.

The optical signal is injected into the FP-LD and would experience the FP etalon effect in the FP cavity. When the wavelength of the optical carrier is located at one of the transmission peaks of the FP cavity, the FP cavity works as a low-pass filter. The high frequency components of the injected signal are filtered out. By considering the FP etalon effect, the optical signal at the output of the cavity can be rewritten as

$$E_2(t) = F^{-1}\{F[E_1(t)] \cdot H(f)\}, \quad (2)$$

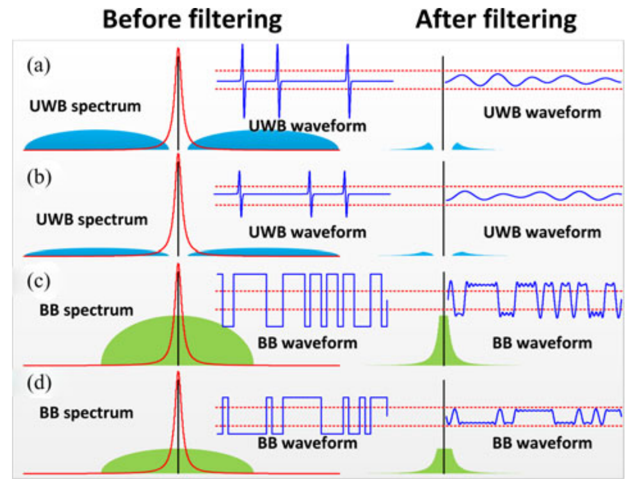

Fig. 2. Illustration of the impact of the FP etalon effect on the injected optical UWB and baseband signals.

where F and F^{-1} denote the Fourier transform and the inverse Fourier transform, respectively, $H(f)$ is the transfer function of the FP cavity.

Fig. 2 illustrates the impact of the FP etalon effect on the injected optical UWB and baseband signals. The powers of the electrical modulation signals are varied to show the results corresponding to different modulation depths or ERs. The red solid line shows the transmission peak of the target mode in the cavity. From Fig. 2(a) and (b), we can see that the UWB signal has most of its power filtered out since most of the frequency components are located at higher frequencies. After filtering, only some low frequency components with very low power remain and the temporal waveform is converted into a quasi-baseband signal with the peak-to-peak amplitude value greatly reduced. When the modulation power increases, the waveform of the filtered signal has small changes, since most of the UWB frequency components are blocked. Therefore, the peak-to-peak amplitude of the filtered UWB signal is not significantly increased when increasing the electrical modulation power.

For the baseband signal, shown in Fig. 2(c) and (d), since most of the power of the baseband signal is located at the low frequency region, a large proportion of the baseband signal power remains after filtering. When the electrical modulation power increases, the peak-to-peak amplitude of the filtered signal also increases. Therefore, the power of the filtered baseband signal increases significantly with the increase of the modulation depth. It should be noted that an FP cavity with high reflectivity at both the front and rear facets has stronger filtering effect than that of an anti-reflection FP cavity whose front facet reflectivity can be as low as 1%. With a high reflectivity at both facets, the 3-dB bandwidth of the transfer function of the FP cavity is much narrower. This, in turn, improves the filtering effect of the cavity. Both the filtered UWB and baseband signals will be less sensitive to the electrical modulation power.

For a semiconductor laser with a given output power, injection locking of the laser is determined by the injection power and the wavelength separation, $\Delta f = f_s - f_i$, where f_s is the injection wavelength and f_i is the free running wavelength. However, a

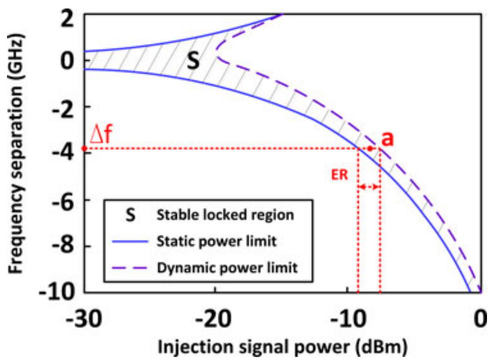

Fig. 3. Injection locking of a semiconductor laser [18]. The output optical power of the semiconductor laser is assumed to be 0 dBm.

strong injection power may lead to relaxation oscillation, thus the injection power should not be too large. To ensure stable injection locking, the injection power must be confined in a region determined by the smallest injection power required to ensure stable injection locking (static power limit) and the maximum injection power limited due to the relaxation oscillation (dynamic power limit) [18]. The static and dynamic power limits can be obtained through finding the stationary solutions of the rate equations of the injection locking system [19], [20]. Fig. 3 shows the relationship between the injection power and the wavelength separation [18]. The solid line gives the region defined by the static power limit. The dashed line defines the border of the relaxation oscillation. Stable operation is ensured if the injection power and the injection wavelength are within the shadowed region.

As can be seen in Fig. 3, the locking wavelength is shifted toward a longer wavelength when the injected power increases (the area formed by the two solid lines is not symmetrical). This is due to the dependence of the refractive index on the carrier density in the cavity active region [21]. For a given wavelength separation, there exists an interval of the injection power. This interval sets the limit for the minimum and maximum powers of the injection signal, corresponding to the peak-to-peak amplitude or the ER of the injection light. For a different frequency separation, a different ER is required. Point a in Fig. 3 marks the average optical power of the injected signal for a given wavelength separation. Mathematically, the power of the filtered signal is given by $P_2(t) = |E_2(t)|^2$. To achieve stable injection locking, $P_2(t)$ should satisfy $P_{\mathrm{dynamic}} > P_2(t) > P_{\mathrm{static}}$, where P_{static} and P_{dynamic} are the power limits set by the static and dynamic limits at a given frequency separation Δf, respectively. This condition also indicates that the input optical signal sent to the FP cavity should have a relatively low ER, i.e., the modulation depth of the downstream signal should not be too high.

Based on the above analysis, the connection between the acceptable maximum electrical modulation power and the stable injection locking can be established. As is shown in Fig. 2, the red dotted line marks the acceptable ER of the injected light. For a UWB signal with different electrical modulation power, the maximum and minimum power of the injected light into the target mode of the FP-LD does not change significantly due to the filtering, as shown in Fig. 2(a). For the baseband signal, as the modulation power increases, the ER of the filtered signal increases more rapidly than that of the UWB signal, and would exceed the ER limit, as shown in Fig. 2(c). Therefore, when the UWB and baseband signal have an identical modulation power, the UWB signal can achieve more stable injection locking as the electrical modulation power increases. The utilization of the UWB signal for injection locking enables the downstream signal to have a higher modulation depth without a severely negative impact on the performance of the upstream service, thus would significantly improve the downstream service performance as well. Through the analysis and comparison, the conclusion is notable: with the same electrical modulation power, the UWB signal is much more suitable for injection locking to generate a clear optical carrier for upstream data transmission. To achieve the same result as the UWB signal, the modulation power of the baseband signal has to be largely reduced. This would in turn lead to worse receiver sensitivities for the downstream service.

Note that the polarization variations during the optical transmission will have impact on the performance of the system. A solution is to use a polarization stabilizer at the receiver. The use of a polarization stabilizer to compensate for the polarization fluctuations has been proposed and employed in polarization-multiplexed transmission systems [22]. In our proposed system, polarization stabilizers should be placed at the base station (BS) and the central station (CS) right after the fiber transmission link.

III. Experiment

The proposed wavelength reuse scheme in a UWB over WDM-PON system is experimentally demonstrated. The experimental setup is shown in Fig. 4. At the CS, a CW light wave at 1553.079 nm from a TLS is equally divided into two parts, and intensity modulated at MZM1 and MZM2 by a baseband signal and a UWB signal, respectively. The baseband signal is a 10 Gb/s PRBS non-return-to-zero (NRZ) signal, generated by a BER tester (BERT, Agilent 4901B); the UWB signal is a 1.25 Gb/s PRBS bi-phase modulation (BPM) UWB signal, generated by an arbitrary waveform generator (AWG, Tektronix AWG 7102). The polarization states of the two intensity modulated signals are adjusted by two PCs to make them orthogonally polarized and aligned with the principal axes of a polarization beam combiner (PBC1). The polarization multiplexed downstream signal is then transmitted through a 25-km SMF (Corning SM28) to the BS. At the BS, the downstream optical signal is sent to a polarization beam splitter (PBS1) via a PC (PC5), to have the signal polarization de-multiplexed. The baseband signal is sent to the upper channel, which is detected by a PD (PD1) (Model 1414, 25 GHz IR Photodetector, New Focus) with the BER measured by a BERT. In the lower channel, the polarization de-multiplexed UWB signal is equally divided into two parts. The lower part is detected by a PD (PD2) (Model 1414, 25 GHz IR Photodetector, New Focus) with the BER performance evaluated also by a BERT. The upper part of the optical UWB signal is sent to the FP-LD (Thorlabs S1FC1550) through the OC and PC6 to injection lock one of the longitudinal modes. The

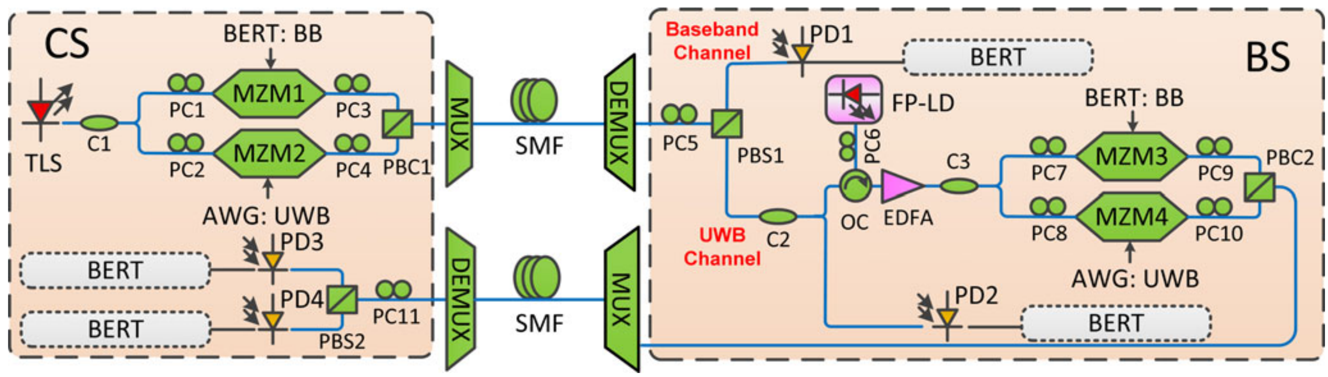

Fig. 4. Experimental setup of the proposed wavelength reused UWB over WDM-PON system.

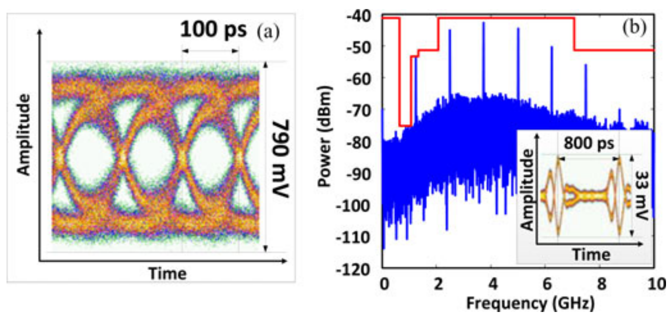

Fig. 5. (a) Measured eye diagram of the received downstream baseband signal and (b) measured electrical spectrum and eye diagram of the received downstream UWB signal.

FP-LD has a threshold current of about 40 mA and is biased at 60 mA to work at the lasing mode. At the output of the FP-LD, a clear optical carrier is generated. An EDFA is then used to amplify the generated optical carrier. The EDFA can be eliminated if an FP-LD with a higher output power is utilized. The generated optical carrier is then used for upstream data modulation and transmission. The upstream signals are a 10 Gb/s NRZ baseband signal and a 1.25 Gb/s on–off keying (OOK) UWB signal, generated by a BERT and an AWG, respectively. Similar to the situation for the downstream service, the optical carrier is equally divided into two parts and each is intensity modulated by an upstream signal at an MZM. The two intensity modulated signals are polarization multiplexed at PBC2. The upstream optical signal is sent to a MUX and then transmitted back to the CS through a 25-km SMF. After being distributed to the CS by the DEMUX, the upstream optical signal is polarization demultiplexed at PBS2. The baseband signal and the UWB signal are then detected by two PDs (Model 1414, 25 GHz IR Photodetector, New Focus) and evaluated by the BERTs to measure the BER performances. Therefore, the symmetric wavelength reused UWB over WDM-PON system is implemented.

The eye diagrams of the received downstream baseband signal and UWB signal are measured and shown in Fig. 5. As can be seen the eyes of the received downstream baseband signal and the UWB signal are widely open. The electrical spectrum of the received downstream UWB signal is also measured; the PSD of the UWB signal meets the FCC spectrum mask for indoor wireless communication.

A comparison experiment using the baseband signal and the UWB signal for injection locking is conducted. As analyzed in Section II-B, the modulation powers of the both signals are set identical. The injection locking results are given in Fig. 6. Fig. 6(a) shows the injection locking using a clear optical carrier, which is used as a reference for comparison. Fig. 6(b) and (c) shows the injection locking using a baseband signal at two different electrical modulation powers. It is clearly seen that when the input modulation power increases, the injection locking performance becomes poorer. The side mode suppression ratio reduces from 35 to 19 dB. Fig. 6(d) and (e) shows the injection locking using a UWB signal at again two different electrical modulation powers. It is clearly seen that the FP-LD is well injection locked for the UWB signal at two different modulation powers. The side mode suppression ratio is kept at 35 dB when the modulation power is increased. The experimental result confirms that the UWB signal is more suitable for injection locking to generate a clear optical carrier. For a baseband signal, injection locking can only be achieved when the electrical modulation power is low; when the electrical modulation power increases, the injection locking is severely deteriorated.

The performance including the BER and the eye diagrams of a 10 Gb/s upstream baseband signal carried by the reused optical carrier from the FP-LD is evaluated when the injection signal is an optical baseband signal or an optical UWB signal at different electrical modulation power levels. Fig. 7 shows the experimental results. As can be seen, the BER performance is superior when the injection signal is a UWB signal. When the electrical modulation power is 19 dBm, the upstream signal can maintain error-free transmission when the injection signal is a UWB signal with a BER of 10^{-9}, but when the injection signal is a baseband signal, the BER is 10^{-3}. Error-free transmission here is defined as the transmission of a signal with a BER no more than 10^{-9}. The eye diagrams for the cases of the two different injection signals are also shown. It is clearly seen that the eye diagrams are kept widely open when the input injection signal is a UWB signal at different power levels. The eye diagram is closed when the input injection signal is a baseband signal, especially at high electrical modulation power levels. This result again confirms that the use of a UWB signal as an injection signal provides better performance for upstream signal transmission. When a baseband signal is utilized for injection locking, the upstream service is sensitive to the downstream modulation depth.

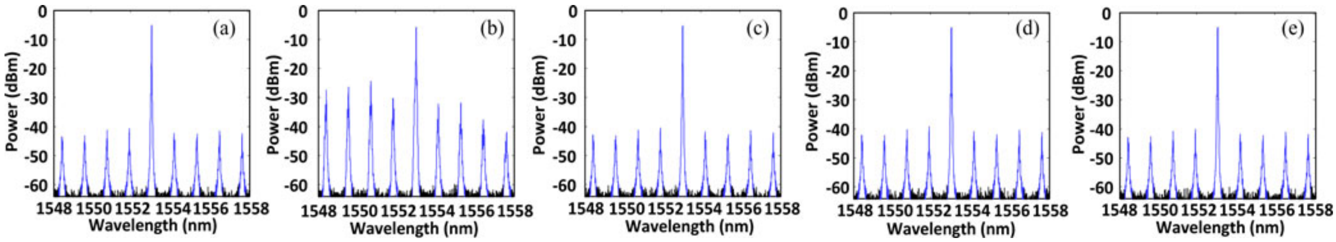

Fig. 6. Measured optical spectrums of the output optical carrier of the FP-LD when the following optical signals are injected: (a) clear optical carrier; (b) 5 Gb/s baseband signal with Pmax; (c) 5 Gb/s baseband signal with Pmin; (d) 1.25 Gb/s UWB signal with Pmax; (e) 1.25 Gb/s UWB signal with Pmin; Pmax: maximum modulation power; Pmin: minimum modulation power.

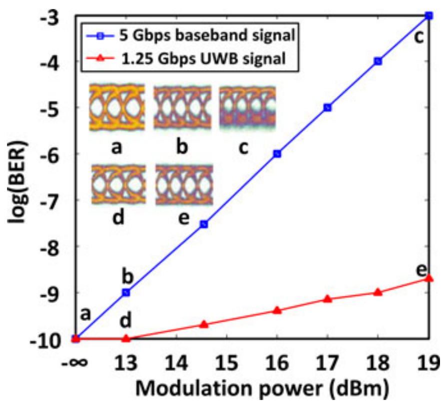

Fig. 7. Measured BER and the eye diagrams of a 10 Gb/s upstream baseband signal for an optical carrier from the FP-LD when the injection signal is an optical baseband signal or an optical UWB signal at different electrical modulation power levels.

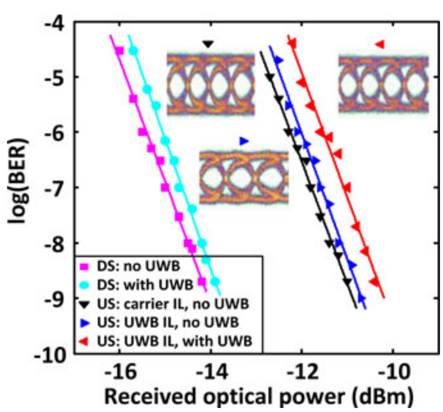

Fig. 8. Measured BERs of the received downstream and upstream baseband signals. Inset: eye diagrams of the received upstream baseband signals.

Through the comparison, the superior performance of using a downstream UWB signal for injection locking over the use of a downstream baseband signal is verified.

Since the use of a downstream UWB signal for injection locking will provide better performance, the system employs the downstream UWB signal as an injection signal for wavelength reuse. The performance of the entire system is then evaluated.

First, the BERs of the downstream and upstream baseband signals are measured. The results are shown in Fig. 8. The eye diagrams of the received upstream baseband signals are also shown in Fig. 8.

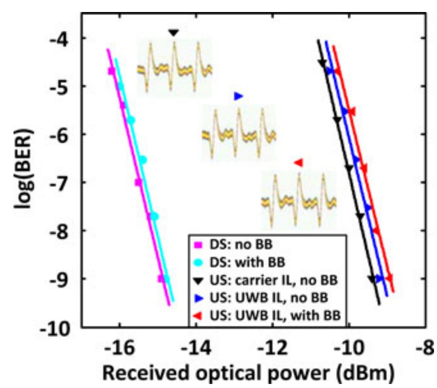

Fig. 9. Measured BERs of the received downstream and upstream UWB signals. Inset: eye diagrams of the received upstream UWB signals.

The BER of the downstream baseband signal is measured without and with a polarization multiplexed UWB downstream signal to study the performance of the polarization multiplexing of the baseband and UWB signals. As can be seen the co-transmission of a downstream baseband and a downstream UWB signal will introduce a small power penalty of 0.3 dB. The effectiveness of the polarization multiplexing is confirmed.

The BER of the upstream baseband signal is then measured. Three different situations are considered: first, the injection signal is a pure optical carrier; second, the injection signal is a UWB downstream signal with no upstream UWB signal (UWB IL, no UWB); third, the injection signal is UWB downstream signal with a polarization multiplexed upstream UWB signal (UWB IL, with UWB). As can be seen that the power penalties caused by the wavelength reuse and polarization multiplexing are as low as 0.2 and 0.3 dB, respectively. The eyes of the upstream signals are also widely open with no obvious deterioration. The good performance of transmissions of both the downstream and upstream baseband signals of the proposed system is verified.

Then, the BERs of the downstream and upstream UWB signals are measured. The results are shown in Fig. 9. The eye diagrams of the received upstream UWB signals are also shown in Fig. 9.

Similar to the measurements for the transmission of the baseband signal given in Fig. 8, the BER of the downstream UWB signal is measured without and with a polarization multiplexed downstream baseband signal to study the performance of the polarization multiplexing. As can be seen, the co-transmission of a downstream baseband and a downstream UWB signal will

TABLE I
POWER BUDGET OF THE PROPOSED UWB OVER WDM-PON

Parameters	Downstream service		Upstream service	
	UWB channel	Baseband channel	UWB channel	Baseband channel
Launch power into fiber link	1 dBm	1 dBm	1 dBm	1 dBm
Fiber link loss	5 dB		5 dB	
Connecter and coupler loss	5 dB	1 dB	1 dB	1 dB
Incident power at receiver	-9 dBm	-5 dBm	-5 dBm	-5 dBm
Receiver sensitivity	-14.8 dBm	-13.9 dBm	-8.9 dBm	-10.4 dBm
CS Minimum launch power: -4.8 dBm			**Power margin: 3.9 dB**	
FP-LD output power: -3 dBm				
EDFA output power: 12 dBm				

introduce a small power penalty of 0.3 dB. The effectiveness of the polarization modulation is again confirmed.

The BER of the upstream UWB signal is then measured. Again, three different situations are considered: first, the injection signal is a pure optical carrier (carrier IL, no baseband); second, the injection signal is a downstream UWB with no upstream baseband signal (UWB IL, no baseband); third, the injection signal is a downstream UWB with a polarization multiplexed upstream baseband signal (UWB IL, with baseband). As can be seen, the power penalties caused by the wavelength reuse and polarization multiplexing are both as low as 0.2 dB. The eyes of the upstream UWB signals are also shown in Fig. 9, which are widely open. The good performance of transmissions of both the downstream and upstream UWB signals of the proposed system is verified.

The receiver sensitivities are also measured. For the downstream BPM UWB signal, the downstream baseband signal, the upstream OOK UWB signal and the upstream baseband signal, the receiver sensitivities are measured to be –14.8 dBm, –13.9 dBm, –8.9 dBm, and –10.4 dBm, respectively. The receiver sensitivity here is defined as the optical power to the receiver required to obtain a BER of 10^{-9} for both the UWB signal and the baseband signal. Note that the receiver sensitivities for the upstream baseband and UWB signals are poorer than those for the downstream signals. This is because the half-wave voltages of the upstream modulators are not high enough, which limits the ERs of the upstream signals. Once the modulators with higher half-wave voltages are utilized, better receiver sensitivities for upstream signals will be attainable.

The power budget of the proposed UWB over WDM-PON is analyzed, which is summarized in Table I. The output powers of the FP-LD and the EDFA are also provided. Due to the low output power of the FP-LD, an EDFA is employed at the BS. However, if an FP-LD with a higher output power is used to replace the current FP-LD for the experiment, the EDFA can be eliminated.

IV. CONCLUSION

A wavelength reuse scheme based on injection locking of an FP-LD and polarization multiplexing for a symmetric UWB over WDM-PON was proposed and experimentally demonstrated. The key contribution of the work was the comparative investigation of the injection locking performance of an FP-LD using a downstream baseband and a UWB signal. It was proved theoretically and experimentally that the use of a UWB signal for injection locking would provide better performance than the use of a baseband signal. Thus, the utilization of a downstream UWB signal for wavelength reuse would enable the downstream signals to have a higher modulation depth without obviously deteriorating the transmission performance of the upstream signals compared with the conventional schemes of injection locking using a baseband signal. Therefore, the proposed UWB over WDM-PON could provide excellent performance for both the downstream and upstream services.

A bidirectional point-to-point transmission of 1.25 Gb/s UWB signal and 10 Gb/s baseband signal over a 25-km SMF was experimentally investigated. The performance including the eye diagrams, the BERs, and the power budget was evaluated. An error-free transmission of both the downstream and upstream services over a 25-km SMF was demonstrated. The power penalties due to the wavelength reuse and the polarization multiplexing were measured to be as low as 0.2 and 0.3 dB, respectively.

REFERENCES

[1] G. R. Aiello and G. D. Rogerson, “Ultra-wideband wireless systems,” *IEEE Microw. Mag.*, vol. 4, no. 2, pp. 36–47, Jun. 2003.

[2] J. P. Yao, F. Zeng, and Q. Wang, “Photonic generation of ultrawideband signals,” *J. Lightw. Technol.*, vol. 25, no. 11, pp. 3219–3235, Nov. 2007.

[3] A. Banerjee, Y. Park, F. Clarke, H. Song, S. Yang, G. Kramer, K. Kim, and B. Mukherjee, “Wavelength-division-multiplexed passive optical network (WDM-PON) technologies for broadband access: A review,” *J. Opt. Netw.*, vol. 4, no. 11, pp. 737–758, Nov. 2005.

[4] G.-K. Chang, A. Chowdhury, Z. Jia, H.-C. Chien, M.-F. Huang, J. Yu, and G. Ellinas, “Key technologies of WDM-PON for future converged optical broadband access networks,” *J. Opt. Commun. Netw.*, vol. 1, pp. C30–C50, Sep. 2009.

[5] S. Pan and J. P. Yao, “Simultaneous provision of UWB and wired services in a WDM-PON network using a centralized light source,” *IEEE Photon. J.*, vol. 2, no. 5, pp. 711–718, Oct. 2010.

[6] L. Y. Chan, C. K. Chan, D. T. K. Tong, F. Tong, and L. K. Chen, “Upstream traffic transmitter using injection-locked Fabry–Pérot laser diode as modulator for WDM access networks,” *Electron. Lett.*, vol. 38, no. 1, pp. 43–45, Jan. 2002.

[7] W. Hung, C. K. Chan, L. K. Chen, and F. Tong, “An optical network unit for WDM access networks with downstream DPSK and upstream remodulated OOK data using injection-locked FP laser,” *IEEE Photon. Technol. Lett.*, vol. 15, no. 10, pp. 1476–1478, Oct. 2003.

[8] F. Xiong, W.-D. Zhong, and H. Kim, “A broadcast-capable WDM-PON based on polarization-sensitive weak-resonant-cavity Fabry–Pérot laser diodes,” *J. Lightw. Technol.*, vol. 30, no. 3, pp. 355–361, Feb. 2012.

[9] S. M. Lee, K. M. Choi, S. G. Mun, J. H. Moon, and C. H. Lee, “Dense WDM-PON based on wavelength-locked Fabry–Pérot laser diodes,” *IEEE Photon. Technol. Lett.*, vol. 17, no. 7, pp. 1579–1581, Jul. 2005.

[10] W. R. Lee, M. Y. Park, S. H. Cho, J. H. Lee, C. Y. Kim, G. Jeong, and B. W. Kim, “Bidirectional WDM-PON based on gain-saturated reflective semiconductor optical amplifiers,” *IEEE Photon. Technol. Lett.*, vol. 17, no. 11, pp. 2460–2462, Nov. 2005.

[11] I. Papagiannakis, M. Omella, D. Klonidis, J. A. Lázaro, A. Birbas, J. Kikidas, I. Tomkos, and J. Prat, “Design characteristics for a full-duplex IM/IM bidirectional transmission at 10 Gb/s using low bandwidth RSOA,” *J. Lightw. Technol.*, vol. 28, no. 7, pp. 1094–1101, Apr. 2010.

[12] T. Y. Kim and S. K. Han, “Reflective SOA-based bidirectional WDM-PON sharing optical source for up/downlink data and broadcasting transmission,” *IEEE Photon. Technol. Lett.*, vol. 18, no. 22, pp. 2350–2352, Nov. 15, 2006.

[13] M. Presi, R. Proietti, K. Prince, G. Contestabile, and E. Ciaramella, "A 80 km reach fully passive WDM-PON based on reflective ONUs," *Opt. Exp.*, vol. 16, no. 23, pp. 19043–19048, Nov. 2008.

[14] L. Chen, H. Wen, and S. Wen, "A radio-over-fiber system with a novel scheme for millimeter-wave generation and wavelength reuse for up-link connection," *IEEE Photon. Technol. Lett.*, vol. 18, no. 19, pp. 2056–2058, Oct. 2006.

[15] Z. Jia, J. Yu, and G.-K. Chang, "A full-duplex radio-over-fiber system based on optical carrier suppression and reuse," *IEEE Photon. Technol. Lett.*, vol. 18, no. 16, pp. 1726–1728, Aug. 2006.

[16] A. Kaszubowska, L. Hu, and L. Barry, "Remote downconversion with wavelength reuse for the radio/fiber uplink connection," *IEEE Photon. Technol. Lett.*, vol. 18, no. 4, pp. 562–564, Feb. 15, 2006.

[17] J. Yu, Z. Jia, T. Wang, and G. K. Chang, "A novel radio-over-fiber configuration using optical phase modulator to generate an optical mm-wave and centralized lightwave for uplink connection," *IEEE Photon. Technol. Lett.*, vol. 19, no. 3, pp. 140–142, Feb. 2007.

[18] S. Yamashita and D. Matsumoto, "Waveform reshaping based on injection locking of a distributed-feedback semiconductor laser," *IEEE Photon. Technol. Lett.*, vol. 12, no. 10, pp. 1388–1390, Oct. 2000.

[19] V. Annovazzi-Lodi, A. Scire, M. Sorel, and S. Donati, "Dynamic behavior and locking of a semiconductor laser subjected to external injection," *IEEE J. Quantum Electron.*, vol. 34, no. 12, pp. 2350–2357, Dec. 1998.

[20] F. Mogensen, H. Olesen, and G. Jacobsen, "Locking conditions and stability properties for a semiconductor lasers with external light injection," *IEEE J. Quantum Electron.*, vol. QE-21, no. 7, pp. 784–793, Jul. 1985.

[21] R. Lang, "Injection locking properties of a semiconductor laser," *IEEE J. Quantum Electron.*, vol. QE-18, no. 6, pp. 976–983, Jun. 1982.

[22] P. Boffi, M. Ferrario, L. Marazzi, P. Martelli, P. Parolari, A. Righetti, R. Siano, and M. Martinelli, "Measurement of PMD tolerance in 40-Gb/s polarization-multiplexed RZ-DQPSK," *Opt. Exp.*, vol. 16, no. 17, pp. 13398–13404, Aug. 2008.

Wentao Cui received the B.Eng. degree in electrical engineering from Tianjin University, Tianjin, China, in 2011.

Since September 2011, he has been a Master of Applied Science Student with the Microwave Photonics Research Laboratory, School of Electrical Engineering and Computer Science, University of Ottawa, Ottawa, ON, Canada. His research interests include photonic generation of UWB signal, wavelength division multiplexed passive optical networks and UWB over fiber technology.

Tong Shao received B.S. and M.S. degrees from Tsinghua University, Beijing, China, in 2007 and 2009, respectively, and Ph.D. degree from Institute National Polytechnique de Grenoble in 2012. He joined the Microwave Photonics Research Laboratory, School of Electrical Engineering and Computer Science, University of Ottawa as a post-doctoral fellow in August 2012. His current research interests include optical communications, radio over fiber technologies, UWB over fiber technologies and microwave photonics.

Jianping Yao (M'99-SM'01-F'12) received the Ph.D. degree in electrical engineering from the Université de Toulon, France, in December 1997. He joined the School of Electrical Engineering and Computer Science, University of Ottawa, Ottawa, Ontario, Canada, as an Assistant Professor in 2001, where he became an Associate Professor in 2003, a Full Professor in 2006. He was appointed University Research Chair in Microwave Photonics in 2007. From July 2007 to June 2010, he was Director of the Ottawa-Carleton Institute for Electrical and Computer Engineering. Prior to joining the University of Ottawa, he was an Assistant Professor in the School of Electrical and Electronic Engineering, Nanyang Technological University, Singapore, from 1999 to 2001.

Dr. Yao has published more than 420 papers, including more than 240 papers in peer-reviewed journals and 180 papers in conference proceedings. He is a Chair of numerous international conferences, symposia, and workshops, including the Vice-TPC Chair of the 2007 IEEE Microwave Photonics Conference, TPC Co-Chair of the 2009 and 2010 Asia-Pacific Microwave Photonics Conferences, TPC Chair of the high-speed and broadband wireless technologies subcommittee of the 2009–2012 IEEE Radio Wireless Symposia, TPC Chair of the microwave photonics subcommittee of the 2009 IEEE Photonics Society Annual Meeting, TPC Chair of the 2010 IEEE Microwave Photonics Conference, and General Co-Chair of the 2011 IEEE Microwave Photonics Conference. Dr. Yao received the 2005 International Creative Research Award at the University of Ottawa. He was the recipient of the 2007 George S. Glinski Award for Excellence in Research. Dr. Yao was selected to receive an inaugural OSA outstanding reviewer award in 2012. He serves as an IEEE distinguished microwave lecturer for 2013–2015.

Dr. Yao is a registered Professional Engineer of Ontario. He is a Fellow of the IEEE, a Fellow of the Optical Society of America, and a Fellow of the Canadian Academy of Engineering.